Characterization of Modern Spacecraft Materials under Space-simulated Environment

Elena Plis[1,8], Miles T. Bengtson[2], Daniel Engelhart[3], Gregory P. Badura[1], Ryan C. Hoffmann[4],

Heather M. Cowardin[5], Jacqueline A. Reyes[6], Alexey Sokolovskiy[4], Timothy R. Scott[7], Jainisha R. Shah[8],

Phoenix Price[9], and Sydney Horne[8]

1. Georgia Tech Research Institute (GTRI), 925 Dalney St NW, Atlanta, GA, 30318, USA
2. National Research Council Research Associateship Program, 3550 Aberdeen Ave., Kirtland AFB, NM, 87117, USA
3. University of New Mexico, Albuquerque, NM, 87106, USA
4. Air Force Research Laboratory, Space Vehicles Directorate, USA, Kirtland AFB, NM, 87117, USA
5. NASA Johnson Space Center, Orbital Debris Program Office, Houston, TX, 77058, USA
6. University of Texas at El Paso, TX, 79968, USA
7. DuPont de Nemours, Inc, Durham, NC 27703, USA
8. Assurance Technology Corporation, Carlisle, MA, 01741, USA
9. George Washington University 2121 I St NW, Washington, DC 20052

Abstract

External spacecraft materials play an important role in satellite protection from the harsh space environment. Research has shown that the physical, chemical, and optical properties of matter change continuously as a result of exposure to solar radiation and aggressive chemical species produced in Earth's upper atmosphere. Thorough knowledge of the material properties evolution throughout a planned mission lifetime helps to improve the reliability of spacecraft. Moreover, the establishment of correlation factors between true space exposure and accelerated space weather experiments at ground facilities enables accurate prediction of on-orbit material performance based on laboratory-based testing. The presented work aims to evaluate the radiation effects of the low Earth orbit (LEO) environment, namely, exposure to the high-energy electrons, atomic oxygen (AO), and vacuum ultraviolet (VUV), on optical properties of several modern spacecraft materials.

Keywords: low Earth orbit (LEO), electron irradiation, atomic oxygen, vacuum ultraviolet, directional hemispherical reflectance, PI, PET.

1. Introduction

The space environment comprises a number of environmental factors, such as different types of ionizing radiation, electrons and protons of various energies, oxygen ions and atoms, micrometeoroids, vacuum, and large temperature fluctuations [1]. Polymer materials used in spacecraft are usually damaged both physically and chemically by these factors thus degrading the functionality of the spacecraft elements and shortening the mission lifetime. Major space weather components related to the degradation of polymers in low Earth orbit (LEO) are atomic oxygen (AO) exposure, vacuum ultraviolet (VUV) exposure, and radiation [2]. The influence of individual LEO-associated hazards, as well as their synergistic effects, should be understood to assist with the selection of proper materials the specific space projects. In-flight materials exposure experiments are the best route for the vetting of material choices, however, due to the high cost and the limited availability of such experiments, as well as the demands for long-duration mission simulations, there is a need for ground-based space-simulated environment facilities to study the space environment effects on materials.

Ground-based simulation of the space environment is experimentally challenging because the space environment varies wildly depending on orbit, solar conditions, and many other factors [3]. Simultaneous exposure of materials to the charged particles, VUV, and/or temperature may be hindered by different acceleration factors for particles and VUV flux, leading to significantly longer VUV irradiation times [4]. Oppositely, once a sequential exposure approach is utilized, materials are exposed to particles (protons, electrons) and VUV, in successive steps, allowing for the separate monitoring of degradation induced by each environmental component.

The total energy provided by solar UV radiation in the range of 100–400 nm is less than 10% of the solar constant, 1366 W/m^2 [5, 6]. VUV effects on polymers are characterized by bond breaking causing degradation of thermo-optical properties, but no direct atomic displacement. On contrary, AO exposure is a severe hazard for polymeric materials. Their interaction with the nominal AO flux at LEO altitudes of $10^{14} - 10^{15}$ atoms/cm^2·second may cause surface erosion, changes in chemical composition and surface morphology, changes in optical properties, and formation of particulate and molecular contamination of the spacecraft surfaces.

Exposure to ionizing radiation strongly depends on the nature of the radiation, its energy, and its dose. High-energy electron bombardment may cause a preferential bond breakage in polymers causing the optical, mechanic, and charge transport properties degradation [7, 8].

Careful characterization of materials' behaviour under simulated space weather conditions in a laboratory environment can inform remote observations, leading to improved identification capabilities and anomaly resolution for space domain awareness (SDA) [9]. Spectroscopic data collected on materials in the laboratory serve as a reference for comparison with orbiting object spectroscopic or photometric data acquired remotely from telescopic systems. Moreover, the same chemical damage that manifests as changes in optical reflectance and absorptance also leads to changes in myriad physical properties such as mechanical strength, electrical conductivity, and chemical reactivity [10, 11, 12]. The correlation of the changes in each of these properties as a function of radiation flux and fluence will allow us to infer a host of material properties based on one experimentally convenient measurement, color change.

This study aims to simulate a LEO environmental material aging in a laboratory setting. To separately examine the effect of each LEO space weather component, a sequential exposure approach was undertaken. Four polymeric materials from the polyimide (PI) and polyethylene terephthalate (PET) families were independently exposed to high-energy electron irradiation, AO atoms, and VUV photons. To monitor a degradation induced by each environmental component, optical properties of the aged materials were accessed.

2. Experimental Details

2.1. Space-simulated Irradiation Procedure

Electron Irradiation

Material irradiation with high-energy electrons as well as the VUV exposure was performed in the Jumbo space irradiation chamber at the Spacecraft Charging and Instrument Calibration Laboratory (SCICL) at Kirtland AFRL [13]. Materials were bombarded with high-energy (100 keV) electrons produced by a mono-energetic Kimball Physics EG8105-UD electron flood gun. According to [8], the mean annual electron flux (>100 keV, electrons, orbit averaged) experienced by the ISS is $\sim 10^{13}$ electrons/cm^2/second. The maximum electron fluence the materials under investigation were exposed to is 8.5 x 10^{13} electrons/cm^2, which corresponds to approximately 10 years at 600-800 km (LEO) orbit, delivered during 5.5 hours. A 24-h vacuum dehydration bakeout was performed on all samples at 60 ◦C prior to radiation exposure to remove any absorbed water. Details of the electron irradiation procedure are reported elsewhere [14].

VUV Exposure

The space-simulated VUV exposure was conducted using three Resonance KrLM-LQD12 lamps installed in the Jumbo chamber at SCICL. The lamp spectrum is composed of 1.0 parts and 2.38 parts of photons with peak wavelengths at 116.5 nm and 123.6 nm, respectively [15]. The photon flux at each wavelength was estimated as 5.5×10^{20} photons/ (seconds · cm^2 · A) at 116.5 nm and 1.06×10^{20} photons/ (seconds · cm^2 · A) at 123.6 nm. Based on Lyman-Alpha flux in-vacuum conversion [16], samples receive an average of 50.9 equivalent sun hours (ESH) per single sample carousel rotation. The expected solar net flux for 6 months of the MISSE-16 mission was calculated to be ~1094 ESH, assuming that ISS completes approximately sixteen 90-minute revolutions per day. The Python code was generated to calculate the angle of each sample relative to the sun according to the orbital beta-angle and ISS position along the orbit. At an average intensity of 50.9 suns, we expect a 6-month simulated aging experiment to be complete in ~ 23 hours.

AO Exposure

Exposure testing of sample materials to an 8 km/s oxygen atom beam was conducted according to ASTM-E2089-15A using the FAST source at the Physical Sciences Inc. The effective peak atomic oxygen fluence during the exposure was calculated using the known witness sample density (Kapton® H, 1.427g/cm^3) and LEO erosion yield of the same material (3×10^{-24} cm^3/O-atom). Effective peak atomic oxygen fluence during the run was 3.1×10^{20} O-atom/cm^2 which corresponds to 6 weeks of LEO exposure. Prior to exposure, all samples were stored in the vacuum chamber for 24 hours to remove water. They were then evacuated and weighed over time to monitor water absorption and allow for the dry mass calculation. Details of the AO-irradiation procedure may be found in [17].

2.2. Materials

The studied materials represent the flight duplicates of samples that were launched as a part of the Materials International Space Station Experiment Flight Facility (MISSE-FF) mission in July 2022. MISSE-FF flight sample collection comprises 14 different materials covering different classes of polymers, including PIs from the Kapton® family, manufactured by E. I du Pont de Nemours and Co., PET materials, liquid crystal polymers, PI/Polyhedral Oligomeric Silsesquioxanes (POSS), and carbon and glass fiber reinforced polymers. This study focuses on two PET materials, Mylar® M021 and Melinex® 454, also manufactured by E. I du Pont de Nemours and Co. and two PI materials from the Kapton family, Kapton TF and Kapton CR, as shown in Table 1.

Table 1. Studied spacecraft polymers.

Material	Abbreviation	Thickness (mil)	Potential application
Mylar M021	PET	10	Improved reflectivity of MLI
Melinex 454	PET	5	
Kapton TF	PI	4	Small satellite parts manufacturing
Kapton CR	PI	2	Sensitive equipment shielding

PET and PI materials are important for the manufacturing of more effective multi-layer insulation (MLI) blankets that are used on the exterior surfaces of spacecraft for the purpose of passive thermal control. These composite materials work by limiting the amount of radiative heat transfer through multiple layers of thin reflectors and spacer materials. An ideal thermal blanket reflects 100% of the incident radiation. In practice, this ideal value has not been obtainable using traditional MLI blankets. Thus, new materials need to be investigated for improved MLI reflectivity and durability. In addition, Kapton CR is a corona-resistant material that may be important for shielding of sensitive equipment on-board a spacecraft, and thermoformable Kapton TF is a possible candidate for small satellite parts manufacturing.

2.3. Characterization

The direct hemispherical reflectance (DHR) of control (pristine), electron-irradiated, and VUV-exposed materials were measured *in situ* during the irradiation procedure according to the optical data acquisition procedure reported elsewhere [18]. Optical properties of AO-exposed materials were characterized using Perkin-Elmer UV/Vis spectrometer within 200 – 2000 nm spectral range. Surface morphology and roughness of studied materials were examined using Bruker Dimension ICON atomic force microscopy (AFM) allowing measurement of surface roughness up to 5 μm on areas as large as 200 μm x 200 μm. Mass loss of AO-exposed materials was measured with 10 microgram accuracy using the microgram balance. Prior to weight measurements, all samples were stored in the vacuum chamber for 24 hours to remove water. They were then removed and weighed over time to monitor water absorption and allow for the dry mass to be calculated.

3. Results and Discussion

Figure 1 presents the DHR spectra of all four studied materials exposed to high-energy electron irradiation with a maximum electron fluence of 8.5 x 10^{13} electrons/cm^2. An absorption band at 830 nm observed in every DHR spectrum is attributed to the partial light absorption in the aluminum of the backing plate.

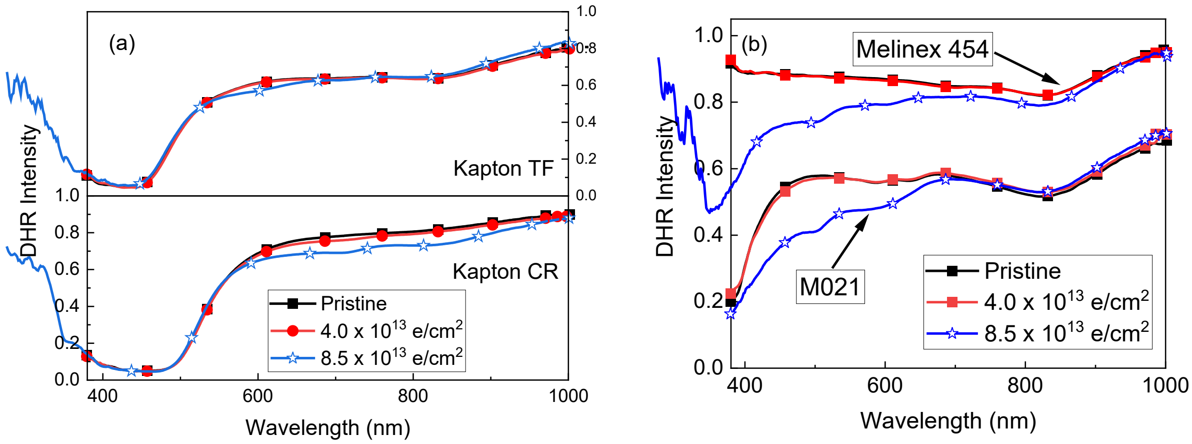

Figure 1. DHR values of pristine and irradiated with high-energy electron PET and PI materials: (a) Kapton CR and Kapton TF, (b) Mylar M021 and Melinex 454.

Kapton TF appears to be the most radiation-stable material since no significant degradation of the DHR signal was observed with an increased fluence of impinging electrons. Kapton CR showed a ~ 7% decrease in DHR signal with irradiation, mainly in the 600 – 900 nm range, which may be due to the radiation-induced formation of shallow trap states within the “bandgap” of the material. Both PET samples were severely affected by the electron bombardment; up to 20% DHR signal reduction was observed in a short wavelength range, 350 – 700 nm. This may be attributed to the radiation-induced condensation of aromatic rings into compact carbonaceous clusters [19].

Figure 2 presents the DHR spectra of control (pristine) and VUV-exposed PET and PI materials in 400-1000 nm spectral range. The prolonged VUV exposure (23 hours) resulted in increased reflectance values of each material in the entire studied wavelength range.

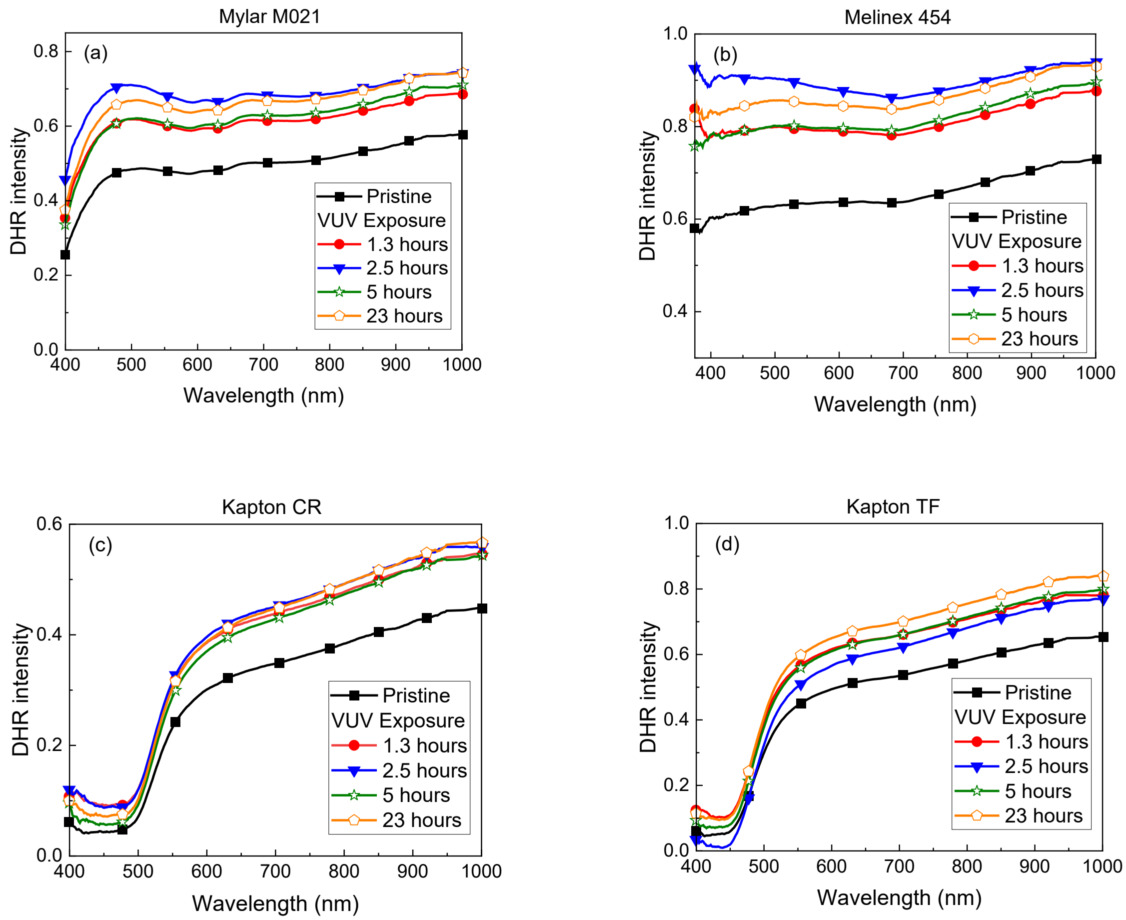

Figure 2. DHR values of pristine and VUV exposed PET and PI materials. (a) Mylar M021, (b) Melinex 454, (c) Kapton CR, and (d) Kapton TF.

The observed reflectance degradation of studied samples may be attributed to the changes in surface microscale smoothness caused by VUV-induced chemical and/or structural changes in polymer surfaces. UV photons are energetic enough to dissociate molecular bonds, resulting in photo-oxidation reactions that scissor or crosslink the polymer chains causing surface morphology modifications. As reported by Qu, *et al.* [20], the surface roughness of VUV-irradiated PI material increases with the dose of the radiation. Similarly, the increased surface roughness of PET films under VUV exposure has been reported [21, 22]. Additional analysis of these samples is necessary to accurately characterize the nature of the chemical changes caused by the VUV exposure.

Figure 3 presents the transmission of control (pristine) and AO-exposed PET and PI materials in the 400-2000 nm spectral range. Light transmission characteristics of all studied materials considerably degraded after

AO exposure, which is attributed to the increased diffuse reflection from the surface roughened by the impinging AO atoms. The surface roughness change of AO-exposed materials compared to their pristine state, as well as mass loss after AO bombardment, are summarized in Table 2. The Kapton TF is the least stable with respect to the bombardment by AO atoms, having the largest mass loss (9.16 mg) and surface roughness increase (130.8 nm) among all of the studies samples.

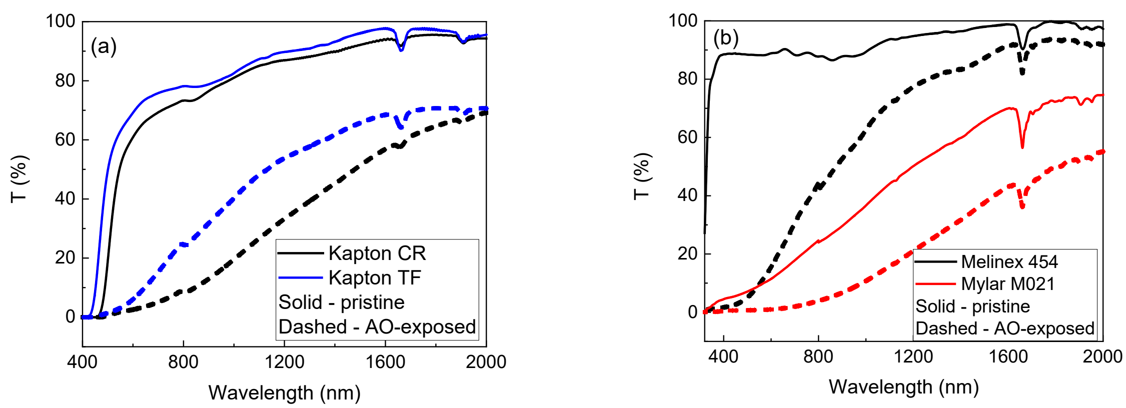

Figure 3. Transmission degradation of PET and PI materials after exposure to AO: (a) Kapton CR and Kapton TF, (b) Mylar M021 and Melinex 454.

Table 2. Mass loss and surface roughness change of AO-exposed materials.

Material	Mass loss (mg)	Surface roughness R_a (nm)	
		Pristine	AO-exposed
Mylar M021	7.89	7.8	187.2
Melinex 454	8.01	8.2	116.7
Kapton TF	9.16	5.5	136.3
Kapton CR	0.84	26.7	62.9

4. Conclusions

Thorough material properties characterization of novel and heritage spacecraft materials during the simulated space weather experiments is important for establishment of correlation factors between true space-exposure and accelerated space weather experiments at ground facilities as well as enabling accurate prediction of on-orbit material performance based on laboratory-based testing. The research presented in this study is part of an effort aimed at developing a complete model of space weather aging that provides a detailed understanding of the damage caused by each of the components of LEO radiation both individually and simultaneously. In particular, the optical properties of four different polymeric materials which may serve in a future MLI design were characterized under LEO-simulated electron irradiation, AO, and VUV exposure performed sequentially. To validate the efficacy of ground-based space weather simulation experiments as well as exposure techniques themselves by the real space observations the same materials were included in material selection for the MISSE-16 experiment launched in July 2022. The space experiment data as well as their comparison with the results of ground experiments will be reported in future publications.

5. Acknowledgements

Authors gratefully acknowledge Physical Sciences, Inc., especially Drs. Daniel M. Hewett and David B. Oakes, for conducting AO-exposure experiments. The authors also would like to thank DuPont de Nemours, Inc., for providing polyimide materials for this research. This work was partially supported by the Air Force Office of Scientific Research, Remote Sensing and Imaging Physics Portfolio (Dr. Michael Yakes) Grant 20RVCOR024 and Georgia Tech Research Institute Independent Research and Development (IRAD) program. One of the authors, P. Price, would like to acknowledge the support of the AFRL Summer Scholars 2022 Program.

6. Disclaimers

The views expressed are those of the author and do not necessarily reflect the official policy or position of the Department of the Air Force, the Department of Defense, or the U.S. government. The appearance of external hyperlinks does not constitute an endorsement by the United States Department of Defense (DoD) of the linked websites, or the information, products, or services contained therein. The DoD does not exercise any editorial, security, or other control over the information you may find at these locations.

Trade names and trademarks are used in this report for identification only. Their usage does not constitute an official endorsement, either expressed or implied, by the National Aeronautics and Space Administration.

References

[1] Lu, Y., Shao, Q., Yue, H., and Yang, F. 2019. A review of the space environment effects on spacecraft in different orbits. *IEEE Access* 7: 93473–93488.

[2] Grossman E., Gouzman I. 2003. Space environment effects on polymers in low earth orbit. *Nucl. Instrum.* 208:48-57.

[3] Gordo, P., Frederico, T., Melício, R., Duzellier, S., and Amorim, A. 2020. System for space materials evaluation in LEO environment. *Advances in Space Research* 66 (2): 307–320.

[4] Duzellier, S., Gordo, P., Melicio, R., Valério, D., Millinger, M., and Amorim, A 2022. Space debris generation in GEO: Space materials testing and evaluation. *Acta Astronautica* 192: 258–275.

[5] Standard Solar Constant and Zero Air Mass Solar Spectral Irradiation Tables, ASTM E 490-00a.

[6] Slepm W.S. in: NASA/SDIO Space Environmental Effects Workshop, NASA CP 3035, 1988, p. 425.

[7] Laghari, J. R., Hammoud A. N. 1990. A brief survey of radiation effects on polymer dielectrics. *IEEE Trans. Nucl. Sci.* 37 (2): 1076 – 1083.

[8] Plis, E. A., Engelhart, D. P., Cooper, R., Johnston, W. R., Ferguson, D., Hoffmann, R. 2019. Review of radiation-induced effects in polyimide. *Appl. Sci*. 9(10): 1999 – 2010.

[9] Hostetler, J., Cowardin, H. 2019. Experimentally-Derived Bidirectional Reflectance Distribution Function Data in Support of the Orbital Debris Program Office. In AMOS 2019 Conference Proceedings.

[10] Plis, E., Engelhart, D. P., Barton, D., Cooper, R., Ferguson, D., and Hoffmann, R., 2017. Degradation of polyimide under exposure to 90 keV electrons. *physica status solidi (b)* 254 (7): 1600819 – 1600826.

[11] Rahnamoun, A., Engelhart, D. P., Humagain, S., Koerner, H., Plis, E., Kennedy, W. J., Cooper, R., Greenbaum, S. G., Hoffmann, R., and van Duin, A. C. 2019. Chemical dynamics characteristics of Kapton polyimide damaged by electron beam irradiation. *Polymer* 176: 135–145.

[12] Mishra, R., Tripathy, S., Dwivedi, K., Khathing, D., Ghosh, S., Müller, M., and Fink, D. 2003. Spectroscopic and thermal studies of electron irradiated polyimide. *Radiat. Meas*. 36 (1): 621–624.

[13] Cooper, R., and Hoffman, R. 2015. Jumbo space environment simulation and spacecraft charging chamber characterization," Tech. rep., Air Force Research Laboratory, Space Vehicles Directorate Kirtland AFB.

[14] Engelhart, D. P., Plis, E., Humagain, S., Greenbaum, S., Ferguson, D., Cooper, R., and Hoffmann, R. 2017. Chemical and electrical dynamics of polyimide film damaged by electron radiation. *IEEE Trans. Plasma Sci*. 45 (9): 2573–2577.

[15] Resonance KrLM-LQD12 lamp brochure. Available at:

https://resonance.on.ca/index_htm_files/LampComparisonBrochure.pdf

[16] Lean J. L., Skumanich A. 1983. Variability of the Lyman alpha flux with solar activity. *J. Geophys. Res*. 88(A7): 5751-5759.

[17] Plis, E., Bengtson, M., Engelhart, D. P., Badura, G., Scott, T., Cowardin, H., Reyes, J., Hoffmann, R., Sokolovskiy, A., Ferguson, D. C., Shah, J., Horne, S. 2022. Characterization of novel spacecraft materials under high energy electron and atomic oxygen exposure. In *AIAA SCITECH 2022 Forum*, p. 0797.

[18] Bengtson, M., Maxwell, J., Hoffmann, R., Cooper, R., Schieffer, S., Ferguson, D., Johnston, W. R., Cowardin, H., Plis, E., and Engelhart, D. 2018. Optical characterization of commonly used thermal control paints in a simulated GEO environment. In AMOS 2018, p. 33.

[19] Steckenreiter T., Balanzat E., Fuess H., Trautmann C. 1997. Chemical modifications of PET induced by swift heavy ions. *Nucl. Instrum*. 131(1-4):159-66.

[20] Qu C., Hu J., Liu X., Li Z., Ding Y. 2017. Morphology and mechanical properties of polyimide films: the effects of UV irradiation on microscale surface. *Materials* 10(11):1329-1328.

[21] Zhang Z. Y., Boyd I. W., Esrom H. 1996. Surface modification of polyethylene terephthalate with excimer UV radiation. *Surf. Interface Anal*. 24(10): 718-22.

[22] Peng G., Yang D., He S. 2006. Effect of VUV radiation on properties and chemical structure of polyethylene terephthalate film. In *Protection of Materials and Structures from the Space Environment*, pp. 225-232. Springer, Dordrecht.